

A First Look into the Structural Properties and Resilience of Blockchain Overlays - Extended

ARISTODEMOS PAPHITIS, Cyprus University of Technology, Cyprus

NICOLAS KOURTELLIS, Telefonica Research, Spain

MICHAEL SIRIVIANOS, Cyprus University of Technology, Cyprus

Blockchain (BC) systems are highly distributed peer-to-peer networks that offer an alternative to centralized services and promise robustness to coordinated attacks. However, the resilience and overall security of a BC system rests heavily on the structural properties of its underlying peer-to-peer overlay. Despite their success, BC overlay networks' critical design aspects, connectivity properties and network-layer inter-dependencies are still poorly understood.

In this work, we set out to fill this gap and study the most important overlay network structural properties and robustness to targeted attacks of seven distinct BC networks. In particular, we probe and crawl these BC networks every two hours to gather information about all their available peers, over a duration of 28 days. We analyze 335 network snapshots per BC network, for a total of 2345 snapshots. We construct, at frequent intervals, connectivity graphs for each BC network, consisting of all potential connections between peers.

We analyze the structural graph properties of these networks and compare them across the seven BC networks. We also study how these properties associate with the resilience of each network to partitioning attacks, i.e., when peers are selected, attacked and taken offline, using different selection strategies driven by the aforementioned structural properties. In fact, we show that by targeting fewer than 10 highly-connected peers, major BCs such as Bitcoin can be partitioned into disjoint, i.e., disconnected, components. Finally, we uncover a hidden interconnection between different BC networks, where certain peers participate in more than one BC network, which has serious implications for the robustness of the overall BC network ecosystem.

1 INTRODUCTION

The widespread adoption of Bitcoin helped the further development of numerous cryptocurrencies and distributed ledger platforms, also known as blockchains (BC). In fact, the unique features of BC's have increased this technology's visibility and are expected to bring disruptive innovation to many sectors that traditionally rely on centralized, trusted third-parties. This, in turn, raises the question of whether their transport layer infrastructure ensures sufficient resilience and performance.

BCs use structured or unstructured peer-to-peer (P2P) networks that employ stateful connections. Such P2P overlays are easily constructed, enable fast distribution of information, and exhibit highly dynamic network topologies. BC-based applications are highly depended on these overlay networks. The overlay network's properties define the level of security, scalability, and resilience of the BCs. It is therefore important to analyze these networks to unveil possible limitations and vulnerabilities. Unfortunately, BC networks are not sufficiently documented by the various BC development teams. Though previously suggested methods had substantial accuracy in topology inference [15, 24, 40, 43, 45], they were usually accompanied by ethical issues since they involved fabrication of double-spending, or otherwise fake transactions that could influence a BC network and have a negative impact on real users' transactions. In addition, frequent changes in the code-base of BC reference clients render past methods for inferring BC network topologies impractical. Similarly, works that rely on simulators [44, 46] are also affected by code-base changes, since the simulation parameters are often tied to the specific implementation.

Authors' addresses: Aristodemos Paphitis, Cyprus University of Technology, Limassol, Cyprus, am.paphitis@edu.cut.ac.cy; Nicolas Kourtellis, Telefonica Research, Barcelona, Spain, nicolas.kourtellis@telefonica.com; Michael Sirivianos, Cyprus University of Technology, Limassol, Cyprus, michael.sirivianos@cut.ac.cy.

In summary, prior work focusing on the specific subject of topology inference has the following drawbacks: a) they largely rely on undocumented subtleties of the reference client; b) they require the monitoring node to be highly connected in the network; c) the monitoring entity has to bear the induced costs of fabricated transactions; d) the current state of BC networks may have changed significantly since a study was done¹; e) they have not studied in-depth the structural properties of BC network layers. Therefore, we identify a first urgent need to study BC networks' structural properties due to their impact on the viability of their BC applications, but this study must be done in a practical, ethically correct, and accurate fashion.

Indeed, the ability to infer the connectivity between BC nodes with sufficient accuracy is required to analyze a network's properties. Yet, due to security concerns, BC networks are built in a way that hides their topology. In fact, knowledge of the topology can enable deanonymization of user transactions, node eclipsing attacks [26, 36], network partition attacks, and create distrust in the system. Past work on BC attacks assessed the vulnerabilities stemming from BC nodes being colocated in just a few Autonomous Systems (AS) or Internet Service Providers (ISP) [2, 49]. This spatial concentration of nodes within an AS or an ISP makes them vulnerable to routing attacks such as BGP hijacking. Such attacks target specific nodes in order to cause significant delays or partition them from the rest of the network.

These attacks have gained attention and are quite practical, since they do not depend on the BC topology. Nevertheless, the success of such attacks requires a powerful adversary, with sufficient hashpower, or the ability to control an AS or ISP. Thus, we identify a second urgent need, i.e., the systematic study of BC overlay networks' topological robustness. Such study involves identifying several critical BC nodes whose removal can cause major disruption. Using partial knowledge of the topology and its structural weak points, an informed adversary may be able to disrupt the BC networks' operation at a relatively low cost.

Motivated by these two urgent needs outlined earlier, our present study focuses on the following three main Research Question (RQ) clusters:

- RQ1:** What are the structural and network characteristics of BC overlay networks? Are all BC networks structured similarly? Do they exhibit properties similar to well-known networks?
- RQ2:** Are there network entities (peers, links) that participate in more than one network, concurrently? What are their properties in comparison to entities appearing in only one network?
- RQ3:** How BC networks evolve longitudinally?
- RQ4:** What are the implications of networks' properties with respect to resilience against targeted attacks? How do concurrent network entities affect network resilience to such attacks? What happens when nodes that appear frequently are targeted by an attacker?

With this work, we make the following contributions:

- We propose an alternative method for studying the topology of BC networks. Our implementation does not require high connectivity in each network and is free of transaction processing costs, allowing for greater scalability. Similar to [40], our work does not interfere with transactions and only uses information made available by the network peers.
- We use our methodology to measure and analyze the network characteristics of seven different BC overlay networks for a period of 4 weeks.
- Our results show that the studied BC networks are not structured in the same way and are highly dynamic in nature. They belong to the general exponential family of graphs, but do not relate considerably to well-known networks like the Internet topology, the Web or social networks and don't resemble random networks either.

¹e.g., number of reported reachable Bitcoin peers has increased roughly by 70% from 2016 to 2020 [6, 18]

- Our results also indicate a significant amount of nodes participating in more than one BC, at the same time. We refer to them as *overlapping nodes*, and show that their presence is high, consistently through time and across major BC. Overlapping nodes constitute 10-40% of any BC network, forming a potential vulnerability in the BC ecosystem, as attackers could focus their effort on the overlapping nodes to disrupt multiple networks simultaneously.
- By performing a longitudinal analysis we discovered that nodes with high up-times are also those with the highest degree. This could be exploited by attackers to identify important nodes in networks that rely on topology hiding techniques for resilience.
- We also investigate the topology robustness of each BC network. We find that by removing just the 5 top central nodes, we get a significant shrinking of the largest connected component in major BCs, suggesting that network partitions can be easily performed by a motivated adversary. We also observe a noticeable increase of the network diameter and dramatic decrease in largest connected component's size when removing less than 10% of peers. Therefore, a powerful DDoS attack, targeting a few hundred nodes, can lead to the collapse of major BC networks.

2 BACKGROUND ON BLOCKCHAIN NETWORKS

This section introduces the seven BC networks considered in our study (Sec. 2.1). It also provides background information on how the two most prominent Blockchain overlay networks are formed (Bitcoin, Sec. 2.2 and Ethereum, Sec. 2.3).

2.1 Studied Networks

We chose seven BC networks for our study. All are consistently included in the top 50 cryptocurrencies by market capitalization, according to [9] for the past year. We list them alphabetically:

- (1) **Bitcoin** [42] was the first cryptographic currency to gain widespread adoption.
- (2) **Bitcoin Cash** [5, 51] is a hard fork of Bitcoin with an increased block size, aiming at increasing transaction throughput and reducing clearance delays in comparison to Bitcoin.
- (3) **Dash** [20] is another fork of Bitcoin. It employs a two-tiered network, consisting of mining nodes and master nodes (peers or nodes are used interchangeably in the rest of the paper). This architecture enables very fast transaction confirmation times.
- (4) **Dogecoin** [38, 59] is a fork of Litecoin (see below), that yields faster (only one minute) block generation times. Although it initially started as a joke to satirize the hype surrounding cryptocurrencies, it has gained visibility and high market capitalization [48].
- (5) **Ethereum** [7] is tailored to executing smart contracts for decentralized applications. It is the most well known cryptocurrency after Bitcoin and has the second highest market capitalization. The main difference with Bitcoin, and its most prominent feature, is the use of a Turing-complete programming language that allows the creation of smart contracts.
- (6) **Litecoin** [34] is one of Bitcoin's first forks. Its differentiating functions include a decreased block generation time of 2.5 minutes and use of a distinct hashing algorithm, Scrypt [47].
- (7) **Zcash** [27] is a cryptocurrency focused on user privacy and anonymity based on zero knowledge proofs for transaction processing.

With the exception of Ethereum, the aforementioned BCs are descendants of Bitcoin using very similar overlay implementations. Next, we explain the fundamentals of the overlay network of Bitcoin and Ethereum.

2.2 Bitcoin Overlay Network

In the Bitcoin overlay network, nodes communicate through non-TLS TCP connections to form an unstructured P2P network. Bitcoin's security heavily depends on the global consistent state of the BC, which relies on its Proof-of-Work based consensus protocol. The communication protocol is largely undocumented, so we look into previous studies and the Bitcoin Core reference client for its specifications. Next, we describe how the Bitcoin network is formed.

When a node joins the network for the first time, it queries a set of DNS seeds that are hardcoded in the reference client (Bitcoin Core). The response to this lookup query includes one or more IP addresses of full nodes that can accept new incoming connections. Once connected to the network, a node receives unsolicited `addr` messages from its connected peers, that contain IP addresses and port numbers of other peers in the network. Additionally, the client can send to peers `getaddr` messages to gather additional peers. The transmitting node can use those IP addresses to quickly update its database of available nodes rather than waiting for new unsolicited `addr` messages. The reply to a `getaddr` message has limited entries and may contain up to a 1000 peer addresses. All known addresses are maintained in an in-memory data structure, and are periodically dumped to disk, in the `peers.dat` file. Bitcoin Core keeps a record of known peers in a persistent on-disk database which allows it to connect directly to those peers on subsequent startups without having to use DNS seeds.

Bitcoin peer address management. For each address in the local database, the client, through the address manager (ADDRMAN), maintains the peer's IP address, port number, last time seen and timestamp of the last connection. If a peer is unreachable, this is marked by the address manager. If multiple attempts to the same peer are unfruitful, the peer is marked as *terrible* [11] and is not tried again. Furthermore, if a peer misbehaves, e.g., by sending invalid blocks, it is also marked as terrible. Terrible peers are not included in `addr` messages. In order to help neighbor selection, all peers are added into buckets. There are two types of buckets: for *tried* and *new* addresses. Peers to which a client had at least one inbound or outbound connection in the past are sorted in *tried* buckets. Peers that are known to a client, but either: a) no connection between them has ever existed, or b) were evicted from a tried bucket, are sorted in *new* buckets. There are 256 *tried* buckets and 1024 *new* buckets. The maximum capacity of each bucket is 64, limiting the total number of peers in the database to 81920.

Topology Inference Risks. To hinder attacks that utilize topology inference, Bitcoin Core developers implemented a series of changes in the network protocol. To address the adversarial methods proposed by Miller *et al.* [40], nodes stopped updating the timestamp field in the address manager, making it impossible to infer most recent, i.e., active connections. Delgado-Segura *et al.* [15] used transaction relay information to infer topology, so the reference client now makes two additional outbound connections that are only used for block relay. This is because inferring network connectivity from the relay of blocks, or block headers, is much more expensive for an adversary. To shield the protocol from node eclipsing attacks, unsolicited `ADDR` messages from incoming peers are now ignored and are not added to the peer's database, nor relayed to other peers. To further reduce the efficacy and impact of eclipsing, peers are selected in a random fashion and updated in fixed time intervals.

2.3 Ethereum Overlay network

Peer protocols. Ethereum's network communication comprises three distinct protocols. *RLPx* serves as a transport protocol and is used for node discovery and establishment of secure communication. *DEVp2p* is used to create the application session. Last, the Ethereum application-level

protocol (eth sub-protocol) facilitates the exchange of BC information between peers, like transactions and blocks. DEVP2P is not meant to be specific to Ethereum; other BC or network applications can be built on it. It supports discovery of other participants and secure communication among them, on top of the RLPx transport protocol. All protocols are documented in Ethereum's official documentation [19].

Node Discovery. Ethereum's node discovery takes place over UDP, while the rest of communication is done through TCP TLS channels. RLPx implements node discovery based on the routing algorithm of Kademlia, a distributed hash table (DHT) [39]. In Ethereum, each peer has a unique 512-bit node ID. A bitwise XOR is used to compute a distance between two Node IDs. Nodes maintain 256 buckets, each containing a number of entries. Each node assigns known peers to a bucket, according to the XOR distance from itself. In order for a new node to find peers, it first adds a hard-coded set of bootstrap node IDs to its routing table. It then sends to these bootstrapping nodes a FIND_NODE message that specifies a random target node ID. Each peer responds with a list of 16 nodes from its own routing table that are closest to the requested target. Subsequently, the node tries to establish a number of connections (typically between 25 and 50) to other peers in the network.

After the peer nodes have discovered other peers through RLPx and a secure TCP connection is established, they use the DEVP2P protocol for communication. Upon exchange of HELLO messages, nodes may use any of the application layers' sub-protocols to communicate. Peers in the Ethereum chain use the eth63/64/65 protocol for exchange of blockchain data after an initial handshake. Ethereum's Node Discovery protocol specification does not allow for repeated discovery messages from the same peer. The Ethereum client implementations impose a 4 second delay between successive FIND_NODE messages from the same node.

3 RELATED WORK

BC Topology Inference. Miller *et al.* [40] were the first to attempt to infer Bitcoin's public network topology. They discovered links between nodes by leveraging the timestamps included in ADDR messages. Before this work, peers responded to GETADDR messages, including a timestamp for each IP address. The timestamp's role was to ensure that terminated nodes were not propagated in the network anymore. The nodes regularly refreshed timestamps. Thus, by issuing GETADDR messages to all reachable nodes in the network and analyzing the timestamps, Miller *et al.* managed to obtain a map of connections. In their work, as in ours, they also find indications that the Bitcoin network is not purely random.

Grundmann *et al.* [24] explored two mechanisms for Bitcoin topology inference. Their first approach exploits the accumulation of multiple transactions before their announcement to other peers but results in a low inference quality. Their second approach exploits the fact that clients drop double-spending transactions. Using this information, they accurately infer a peer's connections. However, this method was not intended to perform full network topology inference due to high cost: with current transaction fees, inferring the connections of a single peer would cost around \$78 [21]. Both methods of [24] require maintaining connections to all reachable peers and crafting distinguishable transactions, one for each reachable peer. Due to ethical reasons, their validation was performed against Bitcoin's testnet.

Delgado-Segura *et al.* [15] devised a different method to infer Bitcoin's network topology, using orphaned transactions. Their method relies on subtleties of Bitcoin's transaction propagation behavior. It involves fabricating double-spending transaction pairs and sending them to a part of the network. Since their method could interfere with ordinary transactions, they have only performed measurements in Bitcoin's testnet. Their results also indicate that Bitcoin's testnet does not resemble a random graph. Using this method with current Bitcoin prices and 11,000 reachable

Bitcoin nodes would require more than \$5,700 in transaction fees and more than 12 hours to cover the whole network [21].

Neudecker *et al.* [45] performed a timing analysis of the propagation of transactions to infer the network topology. In contrast to Miller *et al.*, Neudecker *et al.* use transaction propagation delays, as observed by a highly connected monitor, to infer topology. By observing timestamps of reception of certain transactions and utilizing a propagation delay model, they infer the path of transaction and, thereby, connections between peers. This approach requires the monitoring node to actively create transactions if it cannot determine the transaction originator. Furthermore, changes made to the propagation mechanism of Bitcoin Core reference client render this method impractical.

By exploiting block relay mechanisms, Daniel *et al.* [13] presented a passive method to infer connections of mining nodes and their direct neighbors in the ZCash network. Biryukov *et al.* [4] focused on deanonymizing Bitcoin users by suggesting a method for topology discovery by sending fake marker IP addresses to remote peers. Neudecker and Hartenstein [46] surveyed the network layer of permissionless BCs, simulated a passive method to infer the network topology with substantial accuracy, and emphasized how network topology hiding is an intermediate security requirement. Decker *et al.* [14] measured the rate of information propagation throughout the network and showed, among other findings, that delays in block propagation are highly correlated to chain forks. Finally, work from Dotan *et al.* [17] presents a structured overview of BC P2P overlay networks. Their work highlights differences and commonalities with traditional networks and identifies open research challenges in network design for decentralized distributed systems.

Node Eclipsing and Partitioning Attacks. Heilman and Kendler presented an eclipse attack on Bitcoin's P2P network [26]. They demonstrate how an adversary controlling a large number of IP addresses can monopolize all connections to and from a victim node and exploit it to mount attacks on Bitcoin's mining and consensus. A similar attack has been demonstrated by Marcus *et al.* [37]. It is applicable to the Ethereum BC, and was further optimized in [36]. Saad *et al.* [49, 50] explore various partitioning attacks of the Bitcoin network. Neudecker [44] also explores the feasibility of partitioning attacks through a simulated analysis. Partitioning of the Bitcoin network through BGP hijacks was studied by Apostolaki *et al.* [2]. Such works rely on the spatial concentration of nodes within an AS or an ISP, which makes them vulnerable to routing attacks. More recently, Tran *et al.* [54] proposed a stealthier version of a partitioning attack.

Summary. Despite previous efforts, very little is known regarding the structure and topological properties of BC overlay networks. Instead, past studies focused on methods for inferring the well-hidden topology of Bitcoin, either against the whole network or a specific peer. With the exception of [40], these studies were validated against the Bitcoin testnet [15], or against selected nodes [24, 45].

Topology inference in BC networks remains an unsolved problem. Most suggested methods are either not applicable anymore due to changes in the reference clients, infeasible due to transaction fees, or impractical to run against multiple BC networks since they require maintaining connections to a high number of peers. Furthermore, Bitcoin core developers are constantly updating protocol subtleties to prevent any leakage of information that would ease topology inference in any way.

Contributions. To the best of our knowledge, this is the first study that focuses on various BC networks' structural properties. As we show in Sec. 4.2, we circumvent the challenges of topology inference and build a simple network monitor that can probe seven different BC networks in parallel. We are the first to study these networks in-depth for their network characteristics and properties. Furthermore, we investigate the resilience of these networks against random and targeted attacks.

4 METHODOLOGY

In this section, we explain the methodology used for crawling the aforementioned BC networks (Sec. 4.1), how we assessed the efficacy of our methodology (Sec. 4.2), and the final datasets collected and experimental setup used (Sec. 4.3).

4.1 Crawling Process

To discover the nodes of the overlay networks, we modified the crawler maintained by the popular site *Bitnodes.io* [6] to meet our needs [58]. The required changes included features that enable: a) crawling multiple chains using distinct processes; b) storing the mapping of each node to its known-peers; c) and synchronizing the processes to dump the collected data for each BC at the same timestamp. For Ethereum, which uses a completely different communication protocol, we built our crawler around the open source Trinity client [55]. Our main goal is to scrape the contents of any reachable node's ADDRMAN for its outgoing connections, and to build a connectivity graph of any possible connections that could be realized in the overlay network.

Each BC to be crawled is assigned to a process that creates hundreds of user-level threads. Intermediate data collected during crawling are maintained in an in-memory key-value store, each process having its own instance. Following the communication protocols described in Sections 2.2 and 2.3, each process connects to its assigned BC network and recursively asks each discovered node for its known peers. Each new discovered node is stored in a pending set of the in-memory instance. The threads constantly poll their pending set for a new node, initiate a connection and retrieve the list of the node's known peers.

Upon a successful connection to a peer, its entry is moved from pending to the tried set. Additional data for the peer are collected through the protocol's VERSION message, including provided services, the peer's latest block height, the client's software version, and the peer's P2P protocol version. If a node fails to reply or the connection times out, it is moved into the failed set. On each received reply to a GETADDR message, the program makes an entry, mapping the originating node (N_{or}) to the peer list it knows of: $N_{or} \rightarrow \{P_0, P_1, \dots, P_n\}$, where P_{0-n} are the peers included in N_{or} 's reply. This entry is stored in the edges set.

When the pending set becomes empty, the crawler moves all entries from tried to the pending, and starts over. The edges set remains intact and is updated in subsequent rounds. Replies from nodes that are already mapped in the edge set, are appended to the respective entry. After a period of approximately two hours, all processes synchronize and dump their edge set to storage. Subsequently, after the dump, all sets are emptied and each process restarts and repeats the same procedure. Note that in our implementation, we do not accept incoming connections and we probe only IPv4 peers. Because Bitcoin descendant BC networks share their communication protocol semantics with Bitcoin, only a few constant parameters have to be changed in order to be compatible with our implementation.

Note: The latest version of Bitcoin Core includes changes that affect the proposed approach. The latest version employs cached responses to GETADDR requests. For a period of 24 hours, all GETADDR requests from any peer are served by a fixed ADDR reply containing up to 1000 peers. This further impedes the collection of the contents of ADDRMAN [12]. Inspecting our collected data, we found that replies from the same peer vary significantly, with a Jaccard similarity ~ 0.1 of consecutive replies. An aggregated count of a node's neighbors indicates that up to 15% of its peers are more frequently relayed. As our extended analysis on collected snapshots revealed (see Fig. 2), the vast majority of collected nodes are unreachable. Since we rely on reachable nodes to collect data, we would expect a reduction in both the size and density of the synthesized graphs, narrowing the

view extracted by the proposed methods. Nevertheless, the basic aspects of our approach remain valid and we believe its complete efficacy can be restored with further modifications to the crawler.

Implementing an Ethereum crawler is substantially different. We fork a full client that disables all BC-related processing. We only implement those parts of the protocols necessary to instantiate connections to Ethereum peers and take part in the discovery process. Since a discovery message in Ethereum provides us with up to 16 addresses, we repeat the discovery process for each discovered peer after a 5 second interval, each time generating a new random target (see Sec. 2.3 for details). We note that it is more time-consuming to scrape the DHT contents of each Ethereum peer compared with other BCs.

4.2 Methodology Assessment

We evaluate the efficacy of our method as follows. We setup an unmodified Bitcoin reference node using the official Bitcoin core implementation[10]. After the initial deployment, we allowed the reference node to perform its initial bootstrap of the BC for one week. Subsequently, every ten minutes we retrieve the following information from the reference node: a) all inbound and outbound connections, b) a copy of the `peers.dat` file, containing all known peers, and c) the ADDR reply to a GETADDR probing message. Looking into the collected data, we found:

- After more than one week of operation, the `peers.dat` file of the reference client contained 41k IP addresses.
- Some peers are more frequently included in ADDR replies than others. By sending 20 GETADDR messages, we were able to retrieve 17k unique peers, instead of the expected 20k (1k per message), meaning that a group of nodes appears more frequently than others.
- The number of outgoing connections of the reference client was between 8 and 12. Despite their small number, the IP addresses of most outgoing connections were included in the node's replies.

Imtiaz *et al.* [28] studied churn in the Bitcoin network and showed that the majority of peers stays online for less than a day, and more than 95% of nodes stay online for less than a week. Accordingly, in Figure 1b, we plot the true positives (recall) of outgoing connections being included in an ADDR reply for four consecutive days. On average, the recall is higher than 0.8. We note that for this calculation, we filter out transient connections, i.e., connections that last for less than 2 hours. From the above, we conclude that our earlier proposed method can repeatedly retrieve a good representation of a node's outbound connections. The resulting graphs, synthesized by the edge sets collected, contain the outbound connections of each node with high probability and may be considered as graphs of the overlay network topology. The actual true connections of active nodes would then be spanning sub-graphs of the synthesized graphs, containing all vertices but less edges.

4.3 Datasets & Experimental Setup

We crawled the selected BC networks from the datacenter of a European University. The monitoring server has an 8-core/3.2GHz CPU, 64GB RAM, and 2.1TB of HDD storage. The crawling operations were done for a period of about one month (26/06-22/07/2020). At the end of the crawling period, we had collected 335 network snapshots for each BC network, or 2345 graphs in total. We denote as C the set of BC networks ($c \in C$) that are crawled:

$$C = \{\textit{Bitcoin}, \textit{BitcoinCash}, \textit{Dash}, \textit{Dogecoin}, \textit{Ethereum}, \textit{Litecoin}, \textit{Zcash}\}$$

At the end of every two-hour period, we have seven different edge sets, one per BC in C . All such edge sets are annotated with the timestamp t of their crawl. Each set of edges corresponds to a graph, denoted as S_c^t , representing a snapshot of BC network c , at timestamp t . We construct the

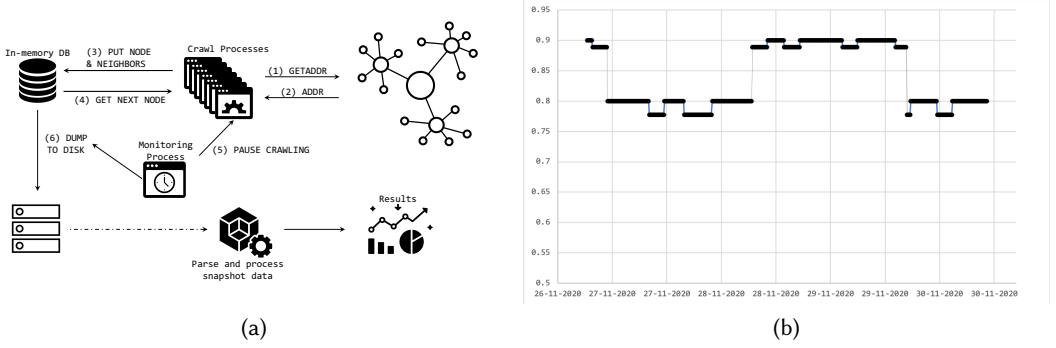


Fig. 1. (a) Data Collection Pipeline, (b)Assessment: Recall of IP addresses.

graphs using the edge sets collected, as follows. For each entry $N_{or} \rightarrow \{P_0, P_1, \dots, P_n\}$ in the set, we create a directional graph with nodes $\{N_{or}, P_0, P_1, \dots, P_n\}$ and add n outgoing edges from N_{or} to nodes P_0, P_1, \dots, P_n . We synthesized and analyzed these graphs using the SNAP library [33] and the NetworkX package for network analysis [25].

A graphical representation of our data collection is depicted in Figure 1a. Steps 1-4 correspond to the crawling process. Steps 5 and 6 represent the synchronized data dump of the collected snapshots from the in-memory database to disk. The bottom part of the figure refers to the analysis of the collected graphs after a pre-processing step.

Summary. In this section, we introduced the methods used to crawl the BC network and to synthesize the collected data into a series of graph snapshots. As described in Section 3, previous methods are either no longer applicable, too costly to perform, or require high connectivity within a network. To be able to explore various networks concurrently, we chose a simpler crawling method that does not require strong presence in a network and does not induce high transaction processing costs. In fact, we performed measurements on seven distinct BC networks from a single server. Our method produces acceptable representations of the real BC overlays. However, we acknowledge that our work will be impeded by changes introduced in the latest Bitcoin Core reference client.

5 RESULTS

In this section, we present the analysis of the collected data per BC network. We begin by analyzing the network properties of the derived graphs and their topological resilience (Sec. 5.1). Furthermore, we investigate whether BC network nodes participate in more than one network simultaneously, and their properties (Sec. 5.2). We study the BC networks' resilience to targeted attacks on specific nodes (Sec. 5.4). Finally, we summarize our findings in Sec. 5.5.

5.1 Networks Structure

This section is driven by Research Question 1. In particular, we are interested in answering the following questions: a) What are the structural properties and network characteristics of BC overlay networks? b) Are they all structured in a similar manner? c) Do they share common properties? d) Do they have properties that relate to other well-known networks such as the Internet topology, the Web, and social networks, or do they resemble random networks?

Basic network properties. The basic properties of the derived graphs are summarized in Table 1. The metrics were computed individually on each graph S_c^t and were then averaged.

Table 1. Basic network graph metrics per BC network. ConnCmpSz: Size of largest connected component (% of total graph); SConCmpSz: Size of largest strongly connected component (% of total graph).

Network:	Bitcoin	Bitcoin Cash	Dash	Dogecoin	Ethereum	Litecoin	Zcash
Nodes	50016	23013	8485	1214	11887	8205	1457
Edges	4793847	169020	7312276	116376	59297	741502	106890
ConnCmpSz	0.99	0.99	1	1	0.99	1	1
SConCmpSz	0.11	0.04	0.82	0.27	0.04	0.16	0.16
Diameter	4	4	4	3	6	4	4
Density	0.0019	0.0003	0.1035	0.0805	0.0006	0.0112	0.0617
Avg. Degree	92.8	7.12	802.12	74.97	4.3	104.04	56.96
Assortativity	-0.2	-0.64	-0.06	-0.13	-0.02	-0.01	-0.22
Reciprocity	-0.06	0.05	0.16	0.34	0	0.09	0.47
Clustering	0.0489	0.011	0.166	0.28685	0.0022	0.07345	0.30939
Av. Shortest Path	2.55	2.82	1.93	1.77	3.78	1.96	1.72

All networks appear to be well-connected given the size of their largest connected component and low diameters. Most networks have a diameter equal to 4. Exceptions are Ethereum having a diameter of 6 and Dogecoin having the smallest diameter equal to 3. Bitcoin is the largest network with more than 50K nodes. Bitcoin Cash and Ethereum follow, having sizes of 23K and 12K nodes, respectively. Dash and Litecoin have similar sizes, close to 8K nodes. The two smallest networks are Zcash and Dogecoin with less than 1.5K nodes.

Moreover, we observe that Dash is markedly the most dense network and is almost fully connected. It has a strongly connected component² comprising 82% of the total network nodes. The large BC networks have a smaller strongly connected component compared to the smaller ones. Table 1 reports the average values of all snapshots. Values extracted from our datasets match reported values in related measurement works [13, 16, 30]. Indicatively, on each day, our monitoring node was able to discover 120081 nodes in Bitcoin, 19543 in Ethereum, and 4132 in Zcash (reporting median values). On average, the monitoring node performed more than 1.3M requests per day, covering all BC networks.

Degree Distributions. The degree (number of links with other nodes) distribution affects many network phenomena, like network robustness and efficiency in information dissemination [3]. In addition, random networks have binomial degree distributions, while in real systems we usually encounter highly connected nodes that the random network model can not account for. In Figure 2, we plot the complementary cumulative distribution (CCDF) of the out-degree of all collected snapshots for all BC networks studied.

We color the snapshots according to their timestamp. Our first observation is that networks such as Bitcoin and Ethereum manifest considerable variability in degree distribution between snapshots. On the contrary, degree distributions in Dash and Dogecoin have less variability (seen by the distance between snapshots). Another interesting observation is that in most BC networks, we have a high fraction of unreachable nodes, either because they are offline or behind NATs. This observation confirms the findings of Wang and Pustogarov [57] who studied the prevalence and deanonymization of unreachable peers. Our results also suggest that these BC network have

²A strongly Connected Component of a directed graph G is a subgraph in which every vertex is reachable from every other vertex.

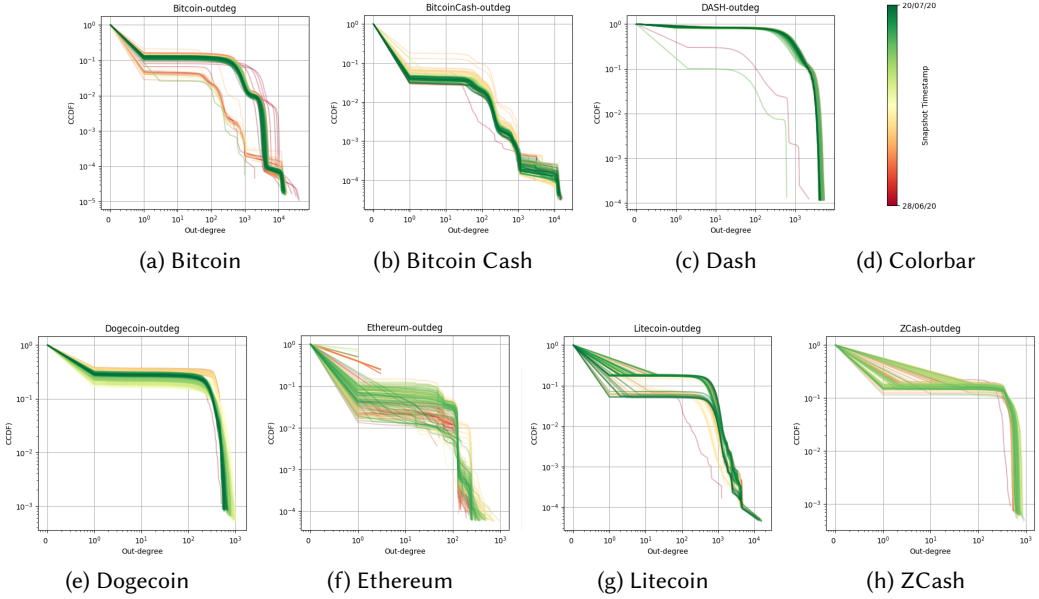


Fig. 2. Out-degree complementary cumulative distribution function of BC networks studied. Snapshots are colored according to the colorbar.

heavy-tailed degree distributions. We further discuss their best distribution fit and their scale-free property in a following paragraph. Finally, we observe significant deviations from the BC protocols. In Bitcoin for instance, one would expect that reachable nodes would have at least 1K out-degree, since Bitcoin clients with the default parameters are set to respond with 1K known peers. Conversely, we observe a number of nodes with out-degree less than 100.

Degree Assortativity. In general, a network displays degree correlations if the number of links between the high and low-degree nodes is systematically different from what is expected by chance. In some types of networks, high-degree nodes (or hubs) tend to link to other such hubs, while in other types, hubs tend to link to low-degree nodes, i.e., what is known as a hub-and-spoke pattern. Assortativity, or assortative mixing is a preference for nodes in a network to attach to others that are similar in some property; usually a node's degree.

The assortativity coefficient, ρ , is the Pearson correlation coefficient of degree between pairs of linked nodes, and lies in the range $-1 \leq \rho \leq 1$. A network is said to be assortative (ρ tends to 1) when high-degree nodes tend to link to each other and avoid linking to small-degree nodes, while low-degree nodes tend to connect to other low-degree nodes. A network is said to be disassortative (ρ tends to -1) when the opposite happens. A random network has ρ close to zero and can be characterized as neutral. The addition of this characteristic to network models approximates better the behaviors of many real world networks.

Correlations between nodes of similar degree are often found in the mixing patterns of many observable networks. For instance, social networks tend to be assortative, while technological and biological networks typically show disassortative mixing, as high-degree nodes tend to attach to low-degree nodes. We compute the assortativity coefficient for each snapshot of BC network and report the average value over all snapshots in Table 1. We find that Dash, Ethereum, and Litecoin

have neutral assortativities. Conversely, Bitcoin Cash, Zcash, and Bitcoin are more disassortative. Negative assortativity reveals a hub-and-spoke structure of these networks, and hints to the existence of central peers that are important in the network.

Out/In Degree Ratio. Link analysis using the in-degree and out-degree distributions has proven very powerful in identifying authoritative and central nodes in the Web and social networks [31]. We computed the out-degree over in-degree ratio of individual nodes for all snapshots and use it to compare the structure of BC networks to the Web and social networks. In the Web, most nodes have considerably higher out-degrees than in-degrees ($\frac{Out}{In} > 1$), while a small fraction of nodes have significantly higher in-degrees than out-degrees ($\frac{Out}{In} < 1$). Social networks have substantial correlation between in-degree and out-degree and most nodes have an in-degree within 20% of their out-degree [41]. In Figure 3, we show the cumulative distributions of the outdegree-to-indegree ratio for nodes in all networks. Dogecoin marginally resembles a social networks with 45% of its nodes having a good correlation, within 20%. This can be explained by the high number of symmetric links, since Dogecoin has the largest reciprocity (see Table 1). In Bitcoin and Bitcoin Cash, most nodes have considerably higher out-degree than in-degree, while a small fraction of nodes have significantly higher in-degree than out-degree, a characteristic similar to the Web. Their resemblance to the Web can be further strengthened by their disassortative nature (see Table 1). In Dash, we cannot observe any correlations, with half the nodes having higher out-degree and the other half having higher in-degree. This indicates that half of the nodes in Dash are frequently online in contrast with the other half that participate periodically. Closer inspection confirms this indication but is omitted due to space considerations. In Litecoin and Zcash, we observe a concentration of nodes having higher out-degrees. Compared with their assortativity, this indicates that these nodes tend to connect to lower degree nodes. In Ethereum, due to its distinguished discovery mechanism, the vast majority of nodes have a very high out- over in-degree ratio.

Reciprocity. Moreover, we measure the reciprocity property, which is a measure of likelihood of vertices in a directed graph to be mutually linked. It has been shown to be critical in modeling and classification of directed networks [23]. Table 1 lists the average reciprocity across all snapshots for each BC network. Zcash, Dogecoin, and Dash have significantly higher reciprocity values. We can attribute this finding to a similar explanation on size and clustering. Closer examination also reveals that these networks have a considerable number of nodes that are frequently online. Nodes that are frequently connected are more likely to connect to nodes that are also frequently connected, driving reciprocity higher.

Clustering Coefficient (CC). The local clustering coefficient CC_i measures the density of links in node i 's immediate neighborhood: $CC_i = 0$ means that there are no links between i 's neighbors, while $CC_i = 1$ implies that each of i 's neighbors link to each other as well. In a random network, the local CC is independent of the node's degree, and average CC, i.e., $\langle CC \rangle$, depends on the system's size with respect to nodes, N . In contrast, measurements indicate that for real networks, e.g., the Internet, the Web, Science collaboration networks, the CC decreases with the node's degree and is largely independent of the system size [3]. The local CC in a random network (CC_{rand}) is calculated as the average degree $\langle k \rangle$ over N , i.e., $CC_{rand} = \frac{\langle k \rangle}{N}$. The average degree of a network is equal to $\frac{2L}{N}$, where L is the number of links. The average CC of a real network is expected to be much higher than that of a random graph.

In Figure 4(a), we compare the average CC of the BC networks with the expected CC for random networks of similar size. As in other real networks, we observe higher CC than expected for a random network, further indicating that BC networks deviate significantly from random networks. In Figures 4(b)-(c), we plot the dependence of the CC on the node's degree for two of the BC

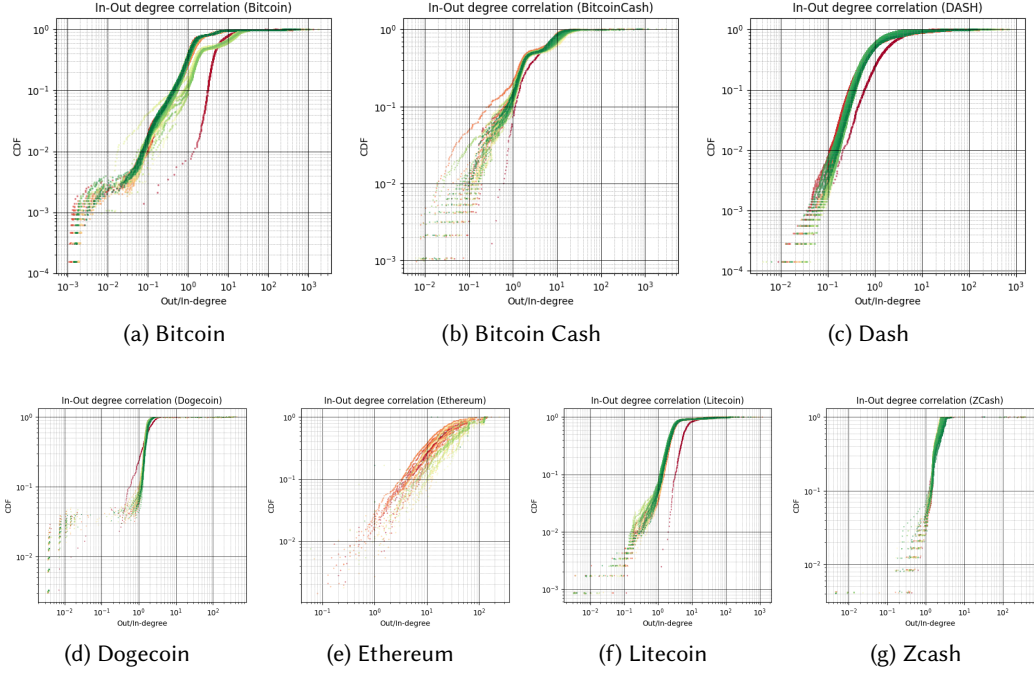


Fig. 3. Cumulative Distribution Function (CDF) of *Out/In* ratio per BC network studied. Snapshots are colored according to Figure 2.

networks under study, where we make some remarkable observations. Although the empirical rule from [3] states that higher degree nodes have lower *CC*, in Bitcoin we observe a significant fraction of high degree nodes with high *CC*. The same finding was observed in Ethereum and Zcash networks as well. Another deviation from the same empirical rule is observed in Dash, where all nodes appear to have an almost constant *CC*, independent of node degree. We attribute this behavior to its temporal characteristics, previously discussed in results related to Fig. 2. Further inspection reveals that Dash has a very low churn, and most nodes are always online. The observed *CC* distributions indicate that BC networks are, in general, governed by rules rarely encountered in other known networked systems.

Scale-free property. One network property tightly related with the degree distribution of a network is the scale-free property. A scale-free network is defined as a network whose degree distribution follows a power law, i.e., having a probability distribution $p(k) \propto k^{-\alpha}$. Exponent α is known as the scaling parameter, and typically lies in the range $2 < \alpha < 3$. The scale-free property strongly correlates with the network's robustness to random failures and has received tremendous attention in the scientific literature (e.g., see [3]). Many real-world networks have been reported to be scale-free, although their prevalence is questioned [8]. To test how well the degree distribution of each BC network snapshot can be modeled by a *power-law* (PL), *log-normal* (LN), *power-law with exponential cutoff* (PLEC) or *stretched exponential* (SE), we calculate the best fit using the *powerlaw* package available by Alstott *et al.* [1].

In Table 2, we report the number of times each type of distribution was the best fit, for all snapshots of the same BC network. The calculated results indicate the dynamic nature of BC

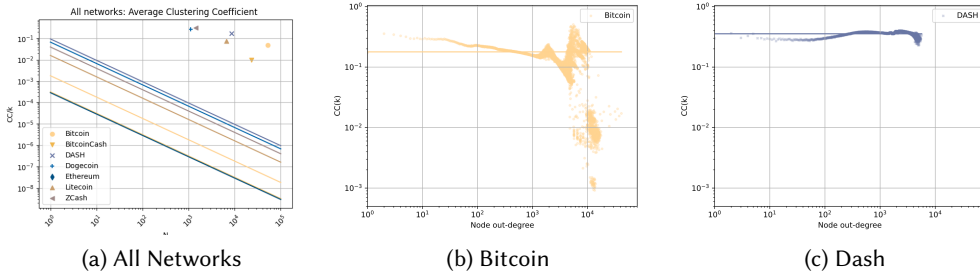


Fig. 4. Analysis of Clustering Coefficient (CC) results.

(a) $\frac{\langle CC \rangle}{\langle k \rangle}$ vs. BC network size; Size and CC averaged across snapshots $S_t^t \forall t \in T$. Markers correspond to the networks of Table 1. Lines correspond to the prediction for random networks, $CC = \frac{\langle k \rangle}{N}$, with constant $\langle k \rangle$ and varying size N . Similar to other known networks, the average CC appears to be independent of the network size N . (b)-(c) The dependence of the local CC on the node's degree for each network. $CC(k)$ is measured by averaging the local CC of all nodes with the same degree k (showing results of aggregating all snapshots of a given BC network). Horizontal lines correspond to the average CC of the network. Other BC networks are omitted due to space limitations.

networks. Such BC networks that change over time may fit different distributions depending on the snapshot collected, something that is also visible in Figure 2. The results suggest that BC networks are not structured in the same way. Nevertheless, their degree distributions, in general, belong to the exponential family of distributions. According to sources [14, 15, 17] Bitcoin's network formation procedure is intended to induce a random graph. Surprisingly, we find that BC networks are substantially different to random networks, confirming past research [15, 40].

Table 2. Degree distributions of BC networks best-fit for different types of exponential distributions. PL: power-law; LN: log-normal; PLEC: power-law with exponential cutoff; SE: stretched exponential.

Distribution	Bitcoin	Bitcoin Cash	Dash	Dogecoin	Ethereum	Litecoin	Zcash
LN	6.29%	76.90%	-	49.40%	21.90%	40.10%	0.60%
PL	0.60%	16.20%	1.80%	4.80%	24.60%	12.60%	18.90%
PLEC	93.11%	6.90%	57.20%	-	18.30%	46.40%	-
SE	-	-	41%	45.80%	35.30%	0.90%	80.50%

Small-world Property. The small-world phenomenon states that if you choose any two individual nodes of a small-world graph, the distance between them will be relatively short, and definitely orders of magnitude smaller than the size of the network. We examined all collected snapshots to see if they satisfy the small-world property, by calculating the ω metric proposed in [53]. The metric is defined as $\omega = \frac{L_r}{L} - \frac{C}{C_l}$ where L and C are the average shortest path and average clustering coefficient of the snapshot, respectively. L_r is the average shortest path for an equivalent random network and C_l is the average clustering coefficient of an equivalent lattice network. The value of ω ranges between -1 , when the network has lattice characteristics, to $+1$ when the network has random graph characteristics, with values near 0 interpreted as evidence of small worldliness.

We did not find evidence that the networks under study satisfy this property. Although we observe low average distances in all BC networks, they do not have high enough clustering coefficients to

Table 3. Edge and Node overlaps (aggregated). ON : number of networks where a unique entity (node or edge) was found to be overlapping, regardless of time

	$ON=2$	$ON=3$	$ON=4$	$ON \geq 5$
Nodes	34814	3909	1489	779
Edges	143577	11034	1958	222

be considered as small-world. Indicatively, the ω values we calculated are greater than 0.5 for Dash and Zcash. The rest of the networks have values greater than 0.8.

5.2 Overlapping Network Entities

In this section, we address the second research question $RQ2$: Are there network entities (peers, links) that participate in more than one BC network, concurrently? What are their properties in comparison to entities appearing in only one network?

Overlaps across time. We define as *overlapping nodes* those nodes that participate in more than one networks at the same timestamp. The intuition of our analysis is as follows. In each snapshot, we compare the set of *overlapping* nodes with all the other nodes, in order to draw insights on *overlapping* nodes' properties. Before describing the details of our study, we outline our mathematical notation to help explain our analysis. As mentioned earlier, the set of BCs studied is C , and the set of all timestamps crawled is T . A snapshot of BC network c , at timestamp t is denoted as S_c^t . We define the set \mathbf{S} as our collected data-set, that consists of all snapshots S_c^t . We denote as S_c^t the subset of \mathbf{S} that contains all networks at timestamp t . Subsequently, for each snapshot $S_c^t \in S_c^t$ we define two groups, G_c^t and $G_c'^t$, such that $G_c^t = S_c^t - G_c'^t$. The first set, G_c^t , is constructed such that $\forall n \in G_c^t, n \notin S_{C \setminus c}^t$. That is, set G_c^t contains the nodes that participate only in blockchain c at timestamp t . Conversely, set $G_c'^t$ contains the *overlapping nodes*; those that participate in blockchain c and at least one other blockchain $c' \in C \setminus c$, at the same timestamp t .

A first approach in finding overlaps between BCs is by looking into our aggregated data-set, \mathbf{S} and count how many nodes and edges (i.e., pairs of endpoints), appear in more than one BC network, regardless of time. Table 3 shows the summary of these results. Evidently, there exists a significant number of network entities (both nodes and edges) that reside in more than one BC network.

A second step is to investigate whether overlapping entities occur frequently or sporadically across time. For this, we focus on the nodes and count all overlapping nodes in each S_c^t . In Figure 5a, for each BC network c , we plot the ratio of $|G_c'^t|$ over $|S_c^t|$, i.e., the number of overlapping nodes in snapshot c over the total number of nodes in the snapshot. We observe that in all BC networks, there is almost a constant percentage of overlapping nodes that join more than one BC network. Therefore, from this and the previous results, we can state that overlaps exist between BC networks, they are significant and occur systematically through time.

Structural Properties of Overlapping Nodes. In this paragraph, we study the properties of overlapping nodes, compared to the rest of the network. The main idea is to check for any differences between sets G_c^t and $G_c'^t$ that can be supported with statistical significance. For the following analysis, we focused on the graph metrics presented in Sec. 5.1. Specifically, and for each BC network, we compared distributions of in-degree, out-degree, betweenness centrality, clustering coefficient, and page-rank. Since we already found that some of these metrics (degree distributions) are highly skewed (see scale-free property fitting paragraph), we perform a normality test on all metrics to decide on the statistical method to be used for the comparison. The normality test confirmed that

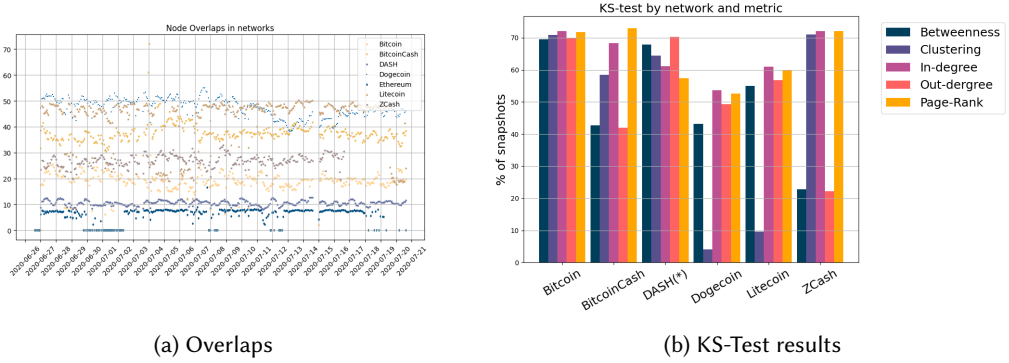


Fig. 5. a) Percentage of nodes that were found in more than one BC network at the same timestamp. X-axis indicates the timestamp. b) Percentage of snapshots where the KS-test indicates a significant distance between the distributions of the overlapping and non-overlapping nodes.

the distributions of all metrics are in fact not normal. Normality was checked by performing the Shapiro-Wilk test, provided by the SciPy package [56]. Since we wish to compare distributions of non-normal data, a non-parametric test is needed. Using the same package, we performed the 2-sample Kolmogorov-Smirnov test (KS-test) between all pairs of G_c^t and $G_c'^t$, for all $t \in T$ and $c \in C$. The KS-test returns the test statistic, D , which is the maximum distance between the cumulative distributions of the two samples. It also returns the p -value for the hypothesis test. If the test statistic D is small, or the p -value is higher than the selected statistical level α (e.g., 0.05), then we cannot reject the null hypothesis that the distributions of the two samples are the same. Our results indicate that in all networks, there is a significant distance between the metrics' distributions among groups G_c^t and $G_c'^t$. Interested to see if there exists a metric that describes this difference better than the others, we looked into our results for the metric that gives significant D values consistently. In Figure 5b, we plot the percentage of all snapshots of a given BC network S_c^t where the p -value of the test is small enough, i.e., p -value < 0.05, and $D > 0.1$. The plot indicates that the distributions between the two groups are often non-equal. We can also observe that in most networks the in-degree and page-rank metrics are the ones found more frequently, meaning that these metrics capture the differences between G_c^t and $G_c'^t$, more often than the other metrics. We also found that the CDFs of overlapping nodes are lower than non-overlapping nodes, meaning that the metrics of overlapping nodes are statistically higher. An exception in this finding was the Dash network (indicated with an * in Fig. 5b), where the opposite is true: in Dash, overlapping nodes have lower metrics than the rest. A key takeaway from this test is that overlapping nodes are in fact different from other nodes. Although this test cannot serve as a proper classifier, it answers our question that overlapping nodes have in fact different properties from the rest of the nodes in a BC network.

5.3 Longitudinal Evolution

Research question *RQ3* asks about the temporal behavior of the BC networks and how they change over time. Permissionless Blockchain networks are open, and nodes may freely come and go. This independent arrival and departure of nodes creates the collective effect known as churn. Churn in Bitcoin has been studied by Imtiaz *et al.* [28]. A recent study by Kiffer *et al.*, explores Ethereum's overlay network in detail, including churn [29]. Stutzbach and Rejaie made an in-depth study of

churn in P2P networks [52]. In their work, they recognize that one of the most basic properties of churn is the *session length* distribution, which describes how long each node participates in the system each time it connects. A *session* begins when a node joins the network and ends when the node disconnects.

In this section, we analyze the node dynamics observed in our collected datasets, focusing on the churn characteristics of the BC networks of interest. Following the methods of [52], we look into the session length distributions.

Limitations As mentioned earlier (see section 4.1), the collected snapshots are two hours apart. All peers that appear in a snapshot are considered to be online for the whole period. This poses a minimum cap to our longitudinal granularity. It does not allow us to capture short-lived connections, i.e., we cannot know whether a node connected and disconnected multiple times within a two-hour period. Since disconnections during a snapshot period are missed, two sessions may look like one longer session. Moreover, very short sessions might not be observed at all, contributing to a bias towards longer-lived connections.

Additionally, due to maintenance operations, snapshots 95 and 253 were not purged to disk in a timely manner (see section 4.1). This resulted in snapshots with duration of six and nine hours, respectively.³ We decided not to include these snapshots in the analysis presented in this section. Furthermore, to better capture any evolution dynamics in, we split our dataset in 4 periods, excluding the two aforementioned snapshots. Each of the four periods has an approximate duration of 5 and a half days:

- *period-0 (p0)*: data from 2020-06-27 to 2020-07-02.
- *period-1 (p1)*: data from 2020-07-03 to 2020-07-08.
- *period-2 (p2)*: data from 2020-07-09 to 2020-07-14.
- *period-3 (p3)*: data from 2020-07-14 to 2020-07-20.

In our longitudinal analysis we decided to use the subset of *reachable peers* of each snapshot, i.e., peers that respond to our requests. This is preferred, since we cannot distinguish between peers that are offline and peers that are alive but behind NATs or firewalls. Finally, during the last days of our measurement period, Zcash's network protocol was updated to a new version, incompatible with the previous one. In effect, we could not capture any node in the Zcash overlay after the 16th of July 2020.⁴

Distribution of Session Length In Figure 6, we plot the complementary cumulative distribution function (CCDF) of session length across the three periods defined above, for each overlay. As can be seen, the distributions for Dash, Dogecoin, Litecoin, and Zcash are very similar for all three periods. This suggests that in these overlays, the distribution of session lengths does not change significantly over time. The distributions for Dogecoin, Litecoin, and Zcash are also similar, suggesting that sessions are consistent across these overlays. In Bitcoin and BitcoinCash, we also observe that session lengths change over time. Nevertheless, across the two systems, the distributions are consistent, with Bitcoin having a small percentage of nodes with sessions longer than BitcoinCash. In Ethereum, we observe that most sessions are short. In fact, fewer than half of the sessions are less than six hours. There exists an obvious shift in session length distribution between the first and the second period, which remains unchanged during the third period. Finally, Dash has the higher percentage of long session lengths with 80% of session lengths lasting for more than 4 days.

Prior studies[28] suggest that session lengths exhibit a behavior similar to a heavy-tailed distribution. To test how well the session length distribution of each overlay can be modeled, we calculate

³ snapshots corresponding to time-stamps 2020-07-03T07:03:22 and 2020-07-14T14:12:12.

⁴ Zcash-Heartwood: <https://z.cash/upgrade/>

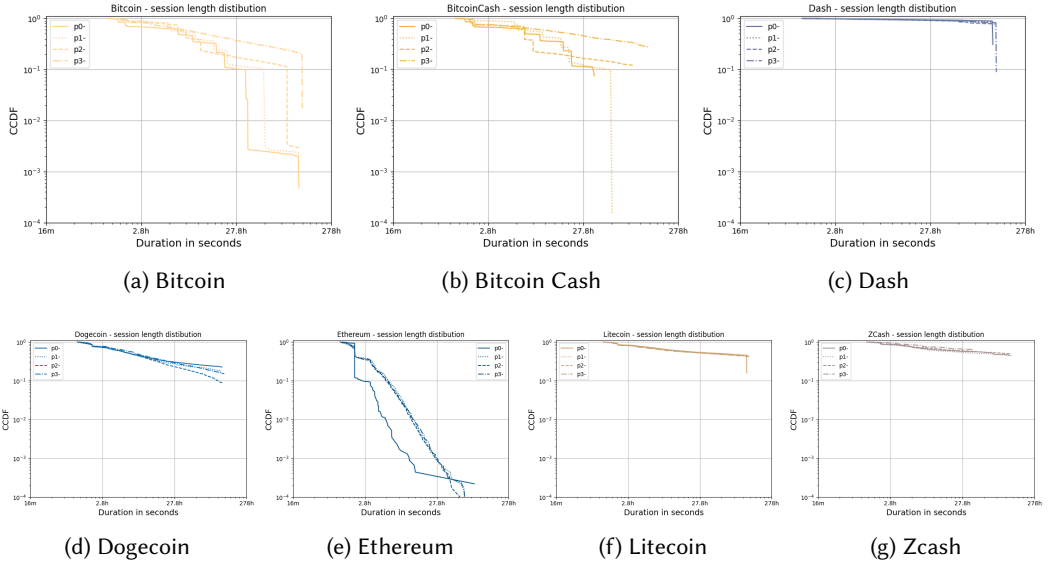


Fig. 6. CCDF of session lengths per BC network studied.

the best fit using the same procedure as in section 5.1, while studying the scale-free property. In Table 4, we report the best fit for each period, for all BC networks. Dash is best modeled by a stretched exponential in all periods, while Dogecoin and Litecoin are best fitted by a power-law with exponential cutoff. The rest of the networks are mostly fitted by a power-law with exponential cutoff.

To summarize, BC networks differ in their temporal characteristics, with a few networks sharing some similarities. The largest networks of our study, namely Bitcoin, BitcoinCash, and Ethereum, have observable differences in their session length distributions between different periods. In these networks, while most sessions are short (less than a day), some sessions are week-long. The observed data in most networks is better described by power-law distributions with exponential cutoff.

Table 4. Session Length best-fit.

PL: power-law; PLEC: power-law with exponential cutoff; SE: stretched exponential.

	Bitcoin	Bitcoin Cash	Dash	Dogecoin	Ethereum	Litecoin	Zcash
period-0	SE	SE	SE	PLEC	PLEC	PLEC	SE
period-1	PLEC	PLEC	SE	PLEC	PL	PLEC	PLEC
period-2	PLEC	PLEC	SE	PLEC	PL	PLEC	SE
period-3	PLEC	PLEC	SE	PLEC	PLEC	PLEC	SE

Correlation between node degree and session length To answer whether node session-length correlates with a node's degree, we calculated the Spearman correlation [32], implemented by the SciPy [56] package. The Spearman rank-order correlation coefficient is a non-parametric measure of the monotonicity of the relationship between two data vectors. In Figure 7a we plot the calculated correlation coefficients between node session-length and node degree for each overlay, per period.

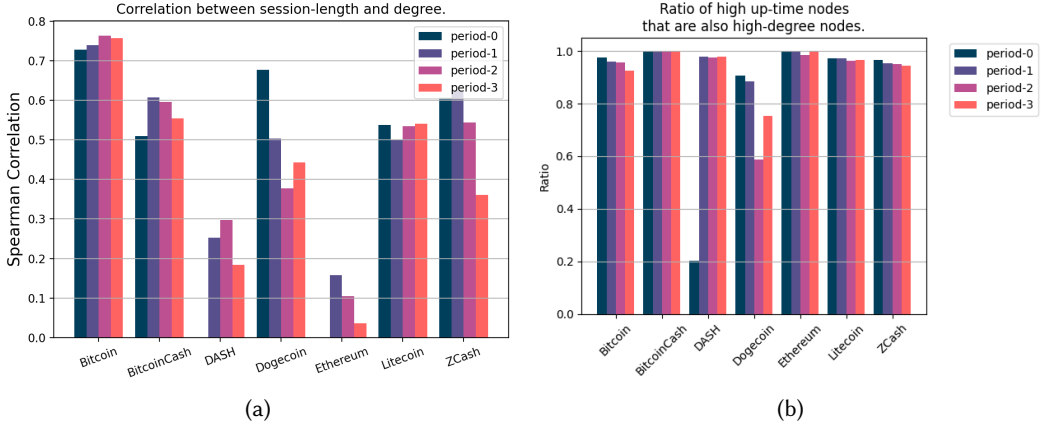


Fig. 7. (a)Spearman Correlation between session-length and node degree. (b) Percentage of high up-time nodes that are also high-degree nodes.

All correlation coefficients are statistically significant with p-values lower than 0.02, except for the first periods of Dash and Ethereum, which are not plotted. The coefficients vary between the four periods and their values point towards moderate to strong correlation in all overlays. In Ethereum and Dash we observe the lowest correlations. We further study the correlation in Ethereum by breaking each period into *low* and *high* degree nodes groups and computing the correlation coefficients per group. The resulting correlation coefficients for higher degree nodes are again positive and higher, between 0.26 and 0.52. The coefficients for the set of lower-degree nodes are negative, indicating a non-linear correlation between up-time and node-degree in Ethereum. Similar observations are made in Dash as well, with high degree nodes having strong positive correlation and low-degree nodes with moderate negative correlation. The relation between up-time and node-degree is further studied in section 5.4

5.4 Network Resilience to Attacks

In this section, we try to answer the third research question, *RQ4*: What are the implications of networks' properties with respect to their resilience against targeted attacks? How do shared (overlapping) network entities affect network resilience to such attacks? Finally, what happens when nodes that appear frequently are targeted by an attacker? To start this investigation, we first describe the attack model. Then, we define four strategies that an attacker could employ to partition a BC network, and we evaluate the efficacy of each strategy.

Attack Model. An adversary may have various incentives to attack a BC system. In this work, we specifically study attacks on the underlying topology of BC networks with the goal to impair the network's main functions. Specifically, we define the following two goals of the attacker.

- (1) **Network partitioning:** to force the BC network into two or more network partitions. A network partition is the decomposition of a network into independent subnets, so that no information flow between the partitions is possible due to the absence of links between nodes.
- (2) **Disturb the information propagation mechanisms** by introducing intolerable delays. Such delays can typically increase the time to reach consensus among all participants and create a

split in the application layer of a BC system. In fact, propagation delays are known to be key contributors towards BC forks [14].

Such attacks would impair a BC network's main functions, potentially causing a decline in users' trust in the system. Attackers with external incentives would be highly motivated to perform such attacks. To measure the efficacy of each goal, we use two metrics: a) the size of the largest weakly connected component, b) the number of connected components, and c) the network diameter. To this end, we take into consideration the following attack strategies:

- (1) Attack minimum-cut edges, in order to partition the network by removing edges that are positioned in key places in the graph.
- (2) Targeted attacks on unique nodes, based on a selected network metric. We test out-degree and betweenness centrality, but others can be employed.
- (3) Targeted attacks on nodes overlapping across more than one BC network. Nodes are ranked on their betweenness centrality.
- (4) Random attacks using random node removals emulate failures that can occur in the network in random fashion and are used as a baseline.

Minimum Edge Cuts. To compute the minimum edge cuts, we used the algebraic connectivity of the derived graphs. The algebraic connectivity of a graph is defined as the second smallest eigenvalue of its Laplacian matrix L , $\lambda_2(L)$ and is a lower bound on node/edge connectivity [22]. Since calculating the algebraic connectivity of a graph is computationally very expensive (i.e., >3 compute hours per snapshot), we analyse one snapshot per BC network. Using the computed eigenvector, we count how many edges are required to be removed to split the network in two parts, and compute their sizes and ratio of the two subnets (cut-ratio, computed as largest subnet over the total). Results are presented in Table 5. Most cuts are heavily unbalanced. Bitcoin Cash has an almost perfect cut, albeit by removing a high fraction of edges (6.5% of edges or 10k edges out of total). Bitcoin and Zcash are somewhat affected, by removing less than 0.5% of their network edges. Overall, targeting minimum cut edges does not have a significant effect in the networks' state and would require the removal (or disruption) of a considerable number of edges connecting nodes.

Table 5. Resilience of BC networks in edge and node removal. Critical Threshold: percentage of nodes that reduce the largest component to 1% of its initial size.

	Bitcoin	Bitcoin Cash	Dash	Dogecoin	Ethereum	Litecoin	Zcash
Edges Removed	5545 (0.1%)	10603 (6.5%)	1451 (0.02%)	581 (0.44%)	2220 (2.71%)	544 (0.08%)	363 (0.33%)
Network Split	9964/ 43949	11367/ 11895	46/ 8556	11/ 1069	436/ 15345	37/ 6576	258/ 1231
Cut Ratio	0.815	0.511	0.995	0.990	0.972	0.994	0.827
Nodes rem.(%) 50% ConCmpSz	5	4	-	-	300	-	25
Nodes rem.(%) #ConCmp > 2	5%	3%	-	-	4%	-	-
Critical Threshold f_c	6.5%	4%	>12%	>12%	5.50%	>12%	>12%

Targeted Node Attacks: Individual BC Networks. We do not study targeted link removals since their removal is usually less effective and more difficult to mount. However, the removal of a node

simultaneously cuts all its adjacent links, and thus, is more efficient from the attacker's point of view. Here, we focus on how to remove nodes in the most efficient way in order to minimize the amount of node removals necessary to cause a disruption. The way a node can be actually removed from the network is out of scope. We follow a static procedure, in the sense that each node is given a priority of removal once and for all, based on a chosen metric. For instance, when using the out-degree metric, the higher the degree, the higher the importance of the node to be attacked. After a node is removed, priorities are not recalculated. Nodes are removed from the network one by one, following the given priority. After each node removal, we calculate the size of the largest weakly connected component and the approximate diameter of the resulting graph. We report the effectiveness of the two node ranking metrics (betweenness centrality and out-degree), and compare with the baseline random removal strategy. We perform the procedure described for all snapshots per BC network. Due to the high number of graphs collected, we stop execution after removing 12% of nodes per snapshot.

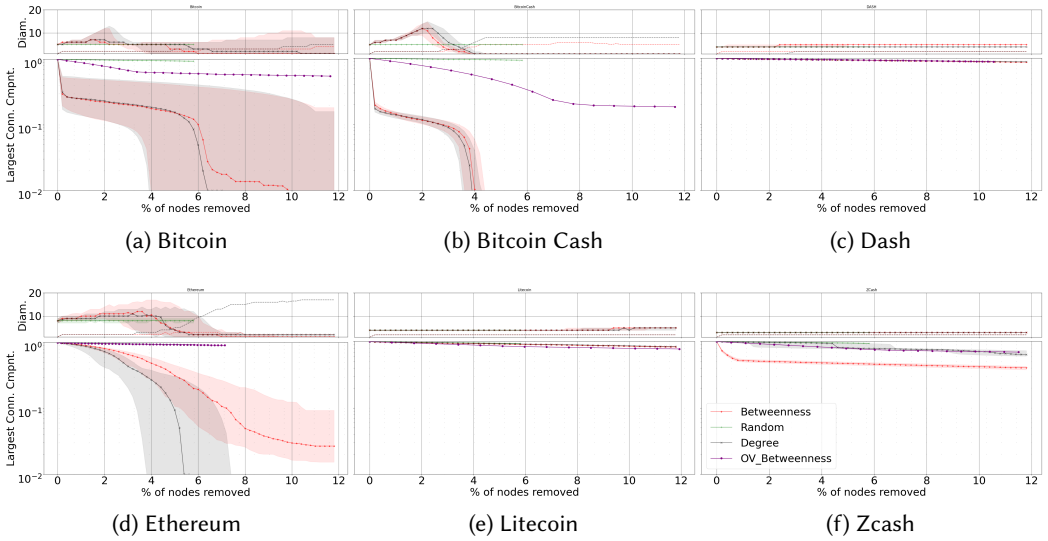


Fig. 8. Evolution of the approximate diameter (upper part) and size of largest weakly connected component (lower part) when the network is under targeted attack. X-axis reports percentage of nodes removed. Dashed lines correspond to number of connected components. Lines correspond to the median value across all snapshots. Shaded area indicates values between 1st-3rd quartile. Red star: Betweenness of unique nodes; Black X: Out-degree of unique nodes; Green +: Random unique nodes; Purple o: Betweenness of overlapping nodes; Dogecoin has a similar shape with Dash and is not included due to space limitations.

In Figure 8 we report our findings. Our first observation is that the connectivity of BC overlay networks is very resilient to random failures. In Bitcoin and Bitcoin Cash, the betweenness and out-degree metrics have roughly the same shape. The size of the largest connected component falls significantly after the removal of just a few nodes. Further removal of nodes shrinks the size gradually until a threshold where the connected component diminishes abruptly to 1% of its initial size. This occurs when removing 6% and 4% of the nodes respectively. Such a behavior is also found in the Internet [35]. This finding may not seem very worrisome, since the percentages reported correspond to a few thousand nodes. Nevertheless, closer inspection of these two networks (not shown in Figure), indicates that the removal of the first 5 nodes, reduces the size of the largest

connected component by 60%, which is alarming. In contrast to the size of the largest component, network diameter starts increasing earlier in this process and has a greater effect in Bitcoin Cash. Dash, Dogecoin and Litecoin seem equally resilient to random and targeted attacks. The size of the largest component drops linearly with the number of nodes removed and their diameter is not significantly affected. We can attribute their resilience to their structural characteristics discussed earlier. Both networks have a very large strongly connected component and high clustering. In Ethereum, the out-degree strategy is more potent. In contrast to Bitcoin and Bitcoin Cash, the size of the largest component does not drop initially. After removing 2% of the nodes, the size drops gradually up to a threshold, close to 5%, where its size falls abruptly to 1%. Network diameter starts increasing early in the process, but not as quickly as in Bitcoin Cash. When targeting high betweenness nodes in Zcash, the largest component falls suddenly at first. Similar to Bitcoin, the first removal of nodes reduces the largest component by 40%. When 4% of the nodes have been removed, the largest component drops to 50% of its initial size, and then it falls almost linearly. Targeting high out-degree nodes is less damaging in Zcash. More than 5% of the nodes need to be removed in order to observe a 20% reduction of the largest component.

Targeted Node Attacks: Overlapping BC Networks. The last part of our research question *RQ3* asks how overlapping nodes can affect resilience of BC networks to targeted attacks. In order to answer this, we repeat the experiment of the previous paragraph with a small variation. From each set $S_{c \in C}^t$, we remove all G_c^t sets. This new set, $S_{c \in C}^t$, contains all nodes that participate in more than one networks at the same time t . We then order the unique elements of $S_{c \in C}^t$, in descending order of their maximum normalized betweenness centrality. Since a node participates in more than one BC networks, we sort nodes based on the maximum value they have across all snapshots at t . We perform normalization using the Min-max method, per snapshot. We then proceed by removing the nodes in $S_{c \in C}^t$ according to their rank, from each snapshot S_c^t at the same time t . Nodes are removed in the same order from all snapshots.

The results of targeting overlapping nodes first, are plotted in Figure 8 using purple circles. The plot reports the average change in the largest connected component over all snapshots S_c^t . Clearly, this strategy is less effective compared to the strategies used earlier, which target top central nodes within a specific BC network. Nevertheless, it provides an adversary the benefit of attacking multiple BC networks simultaneously. One interesting finding is that Litecoin is more susceptible to this kind of attack rather compared to attacks focusing on single BC node metrics. This is partly explained by the fact that Litecoin has one of the highest percentages of overlapping nodes (see Fig. 5a). Closer inspection of the data at hand shows that an attacker is able to shrink the largest connected component of Bitcoin Cash, Bitcoin, Zcash, and Litecoin networks by 70%, 40%, 25% and 20% respectively. This demonstrates that, by targeting overlapping nodes, a powerful adversary can still mount a successful partitioning attack in *4 different networks at the same time*.

Targeted Node Attacks: High up-time nodes. As we have already mentioned in section 5.3, there exists a positive correlation between a node's session-length and its degree. Further inspection of the data revealed that nodes which are connected longer are almost always high-degree nodes. This is somewhat expected as the longer a node is connected, the more peers it is able to discover. In Figure 7b, we plot the ratio of high session-length nodes that are in the top 10% high-degree nodes. For each snapshot, we extract the top 10% nodes ranked by their out-degree. We then set the least up-time of these nodes as a threshold. By selecting the nodes with an up-time longer or equal to that threshold, we calculate the Jaccard similarity of between the two sets of nodes, namely *Long-session nodes* and *High-degree nodes*. This is directly related to our targeted node removal experiment. That is, if we were to repeat the experiment, using a strategy based on nodes' up-time, we would end-up selecting a similar set of nodes with the *highest-degree* strategy already studied.

This leads us to expect similar results in the networks' resilience. The observed relation between a node's up-time and degree could be used to locate nodes of interest in settings that employ topology hiding features, as is the case with the latest Bitcoin reference client (see Section 4.1).

5.5 Key Takeaways

In the preceding paragraphs, we investigated the network characteristics of the BC overlays, and conducted a thorough experimental analysis of our collected data. Furthermore, we studied the presence of overlapping nodes and their properties. Lastly, we investigated several targeted attacks on the connectivity of BC networks. We end this section with a brief summary of important findings we observed in our analysis.

- BC overlays vary significantly in their densities, with larger networks being less dense.
- Their dynamic nature is manifested by the significant variations we encounter in the degree distribution per snapshot.
- Some networks such as Bitcoin Cash, Zcash, and Bitcoin tend to be disassortative, i.e., high-degree peers tend to connect to low-degree peers. Others, like Dash, Ethereum, and Litecoin tend to be neutral in their degree correlations.
- They have low diameters and their average shortest path length is small, i.e., 1.7-3.8 hops. Nevertheless, we did not find evidence that these networks satisfy the small-world property.
- Their clustering coefficient distributions are similar to other real networks, and differ from random networks with similar size and average degree.
- They are well-connected, and their degree distributions belong to the exponential family.
- Some of the collected snapshots can be adequately fitted by a power-law, but most of the time Log-normal, Power-law with exponential cut-off, on Stretched Exponential distributions provide a better fit.
- At all times, a non-negligible amount of overlapping nodes exists between various BC networks.
- We have strong statistical evidence that overlapping nodes differ in their properties and metrics' distributions from the rest nodes within a BC.
- BC overlays are very resilient against random failures. Nevertheless, targeted attacks can have considerable implications on their connectivity. In fact, some networks can be easily partitioned by the removal of less than 10 well-connected nodes.
- Conversely, some BC overlays manifest strong resilience in targeted attacks, that can be attributed to their structural properties.
- A powerful adversary could disrupt at least 4 BC, by targeting overlapping nodes.
- BC overlays have varying temporal characteristics, in terms of session-lengths, and there exists a strong positive correlation between a node's session-length and its degree.

The fact that we do not capture a fully accurate topology of the actual connections between nodes does not diminish the importance of our findings. The results presented in Section 5.4 show a significant portion of all possible connections. In reality, some possible connections may not materialize meaning that the networks may be even less well-connected, which indicates they may be even more vulnerable to partitioning attacks.

6 CONCLUSION

We provide a first and in-depth look into the overlay properties and structural resilience of the seven most prominent, in terms of capitalization, Blockchain networks. We use custom-made Blockchain crawlers to probe 32 million BC peers, obtain each peer's list of known peers, and extract their possible connections. We find that the structure of blockchain networks is unlike that of traditional

networks (e.g., the Web), but shares some similarities. We also find that the graph properties vary substantially among the studied Blockchain networks. Moreover, we discover that, Bitcoin, Bitcoin Cash, Zcash, and Litecoin share a substantial amount of nodes. This fact hints at the efficacy of targeted attacks on a limited set of shared nodes to disrupt more than one networks. At the same time, we find that all networks are robust against random edge removal but some are vulnerable to targeted removal strategies. Moreover, in some networks (Bitcoin, BitcoinCash, and Zcash), the removal of very few nodes results in a significant reduction of the largest weakly connected component's size.

Our results raise the alarm with respect to the resilience of the studied Blockchains against partitioning and message propagation delay attacks. We demonstrate that, by using our methodology, a deliberate and methodical attacker can uncover a small set of entities central to the topology and target them to substantially suppress message propagation in more than one BC network simultaneously. This highlights the need to employ measures to enhance network robustness (e.g., by increasing the number of connections between peers) rather than relying on topology hiding.

7 ACKNOWLEDGEMENTS

This project has received funding from the European Union's Horizon 2020 Research and Innovation program under the Marie Skłodowska-Curie INCOGNITO project (Grant Agreement No. 824015). This work reflects only the authors' views; the Commission is not responsible for any use that may be made of the information it contains.

REFERENCES

- [1] Jeff Alstott, Ed Bullmore, and Dietmar Plenz. 2014. powerlaw: A Python Package for Analysis of Heavy-Tailed Distributions. *PLoS ONE* 9, 1 (Jan 2014), e85777. <https://doi.org/10.1371/journal.pone.0085777>
- [2] Maria Apostolaki, Aviv Zohar, and Laurent Vanbever. 2017. Hijacking Bitcoin: Routing Attacks on Cryptocurrencies. In *2017 IEEE Symposium on Security and Privacy, S&P 2017, San Jose, CA, USA, May 22-26, 2017*. IEEE Computer Society, 375–392. <https://doi.org/10.1109/SP.2017.29>
- [3] Albert-László Barabási et al. 2016. *Network science*. Cambridge University Press.
- [4] Alex Biryukov, Dmitry Khovratovich, and Ivan Pustogarov. 2014. Deanonymisation of Clients in Bitcoin P2P Network. In *CCS*. ACM, 15–29.
- [5] BitcoinCash. 2021. *Bitcoin Cash*. Retrieved 1 Feb 2021 from <https://www.bitcoincash.org>
- [6] bitnodes.io. 2020. *Global Bitcoin Nodes Distribution*. Retrieved 18 Sep 2020 from <https://bitnodes.io>
- [7] Vitalik Buterin. 2014. *Ethereum: A next-generation smart contract and decentralized application platform*. <https://github.com/ethereum/wiki/wiki/White-Paper>
- [8] Aaron Clauset, Cosma Rohilla Shalizi, and Mark E. J. Newman. 2009. Power-Law Distributions in Empirical Data. *SIAM Rev.* 51, 4 (2009), 661–703.
- [9] CoinMarketCap. 2021. *CoinMarketCap*. Retrieved 2 Feb 2021 from <https://coinmarketcap.com>
- [10] Bitcoin Core. 2021. *0.20.1 Release Notes*.
- [11] Bitcoin Core. 2021. *Bitcoin Core, addrman implementation*. Retrieved 2 Feb 2021 from <https://github.com/bitcoin/bitcoin/blob/d0d256536cdfb1443067fb7cc0a19d647f636a5c/src/addrman.cpp#L41>
- [12] Bitcoin Core. 2021. *Cache responses to GETADDR to prevent topology leaks*. Retrieved 2 Feb 2021 from <https://github.com/bitcoin/bitcoin/pull/18991>
- [13] Erik Daniel, Elias Rohrer, and Florian Tschorsch. 2019. Map-Z: Exposing the Zcash Network in Times of Transition. In *LCN*. IEEE, 84–92.
- [14] Christian Decker and Roger Wattenhofer. 2013. Information Propagation in the Bitcoin network. In *13th IEEE International Conference on Peer-to-Peer Computing, IEEE P2P 2013, Trento, Italy, September 9-11, 2013, Proceedings*. IEEE, 1–10. <https://doi.org/10.1109/P2P.2013.6688704>
- [15] Sergi Delgado-Segura, Surya Bakshi, Cristina Pérez-Solà, James Litton, Andrew Pachulski, Andrew Miller, and Bobby Bhattacharjee. 2019. TxProbe: Discovering Bitcoin's Network Topology Using Orphan Transactions. In *Financial Cryptography (Lecture Notes in Computer Science, Vol. 11598)*. Springer, 550–566.
- [16] Varun Deshpande, Hakim Badis, and Laurent George. 2018. BTCmap: Mapping Bitcoin Peer-to-Peer Network Topology. In *2018 IFIP/IEEE International Conference on Performance Evaluation and Modeling in Wired and Wireless Networks*

- (PEMWN). IEEE, 1–6.
- [17] Maya Dotan, Yvonne-Anne Pignolet, Stefan Schmid, Saar Tochner, and Aviv Zohar. 2020. SOK: Cryptocurrency Networking Context, State-of-the-Art, Challenges. In *Proceedings of the 15th International Conference on Availability, Reliability and Security* (Virtual Event, Ireland) (ARES '20). Association for Computing Machinery, New York, NY, USA, Article 5, 13 pages. <https://doi.org/10.1145/3407023.3407043>
 - [18] DSN. 2021. *DSN Bitcoin Monitoring*. Retrieved 1 Feb 2021 from <https://dsn.tm.kit.edu/bitcoin/>
 - [19] Ethereum. [n.d.]. *Ethereum peer-to-peer networking specifications*. Retrieved 1 Feb 2021 from <https://github.com/ethereum/devp2p>
 - [20] Daniel Diaz Evan Duffield. [n.d.]. Dash: A Payments-Focused Cryptocurrency,” <https://github.com/dashpay/dash/wiki/Whitepaper>.
 - [21] Bitcoin Fees. 2021. *bitcoinfees.earn.com*. Retrieved 2 Feb 2021 from <https://bitcoinfees.earn.com>
 - [22] Miroslav Fiedler. 1973. Algebraic connectivity of graphs. *Czechoslovak mathematical journal* 23, 2 (1973), 298–305.
 - [23] Diego Garlaschelli and Maria I. Loffredo. 2004. Patterns of Link Reciprocity in Directed Networks. *Physical Review Letters* 93, 26 (Dec 2004). <https://doi.org/10.1103/physrevlett.93.268701>
 - [24] Matthias Grundmann, Till Neudecker, and Hannes Hartenstein. 2018. Exploiting Transaction Accumulation and Double Spends for Topology Inference in Bitcoin. In *Financial Cryptography Workshops (Lecture Notes in Computer Science, Vol. 10958)*. Springer, 113–126.
 - [25] Aric A. Hagberg, Daniel A. Schult, and Pieter J. Swart. 2008. Exploring Network Structure, Dynamics, and Function using NetworkX. In *Proceedings of the 7th Python in Science Conference*, Gaël Varoquaux, Travis Vaught, and Jarrod Millman (Eds.). Pasadena, CA USA, 11 – 15.
 - [26] Ethan Heilman, Alison Kendler, Aviv Zohar, and Sharon Goldberg. 2015. Eclipse Attacks on Bitcoin’s Peer-to-Peer Network. In *24th USENIX Security Symposium (USENIX Security 15)*. USENIX Association, Washington, D.C., 129–144.
 - [27] Daira Hopwood, Sean Bowe, Taylor Hornby, and Nathan Wilcox. 2020. *Zcash Protocol Specification*. Retrieved 2 Feb 2021 from <https://coinpare.io/whitepaper/zcash.pdf>
 - [28] M. A. Imtiaz, D. Starobinski, A. Trachtenberg, and N. Younis. 2019. Churn in the Bitcoin Network: Characterization and Impact. In *2019 IEEE International Conference on Blockchain and Cryptocurrency (ICBC)*. 431–439. <https://doi.org/10.1109/BLOC.2019.8751297>
 - [29] Lucianna Kiffer, Asad Salman, Dave Levin, Alan Mislove, and Cristina Nita-Rotaru. 2021. Under the Hood of the Ethereum Gossip Protocol. In *Proceedings of the Financial Cryptography and Data Security (FC’21)*. St. George’s, Grenada.
 - [30] Seoung Kyun Kim, Zane Ma, Siddharth Murali, Joshua Mason, Andrew Miller, and Michael Bailey. 2018. Measuring Ethereum Network Peers. In *Internet Measurement Conference*. ACM, 91–104.
 - [31] Jon Kleinberg and Steve Lawrence. 2001. The structure of the Web. *Science* 294, 5548 (2001), 1849–1850.
 - [32] S. Kokoska and D. Zwillinger. 1999. CRC Standard Probability and Statistics Tables and Formulae, Student Edition.
 - [33] Jure Leskovec and Rok Sosič. 2016. SNAP: A General-Purpose Network Analysis and Graph-Mining Library. *ACM Transactions on Intelligent Systems and Technology (TIST)* 8, 1 (2016), 1.
 - [34] Litecoin. 2021. *Litecoin*. Retrieved 2 Feb 2021 from <https://litecoin.org>
 - [35] Damien Magoni. 2003. Tearing down the Internet. *IEEE Journal on Selected Areas in Communications* 21, 6 (2003), 949–960.
 - [36] Yuval Marcus, Ethan Heilman, and Sharon Goldberg. 2018. Low-Resource Eclipse Attacks on Ethereum’s Peer-to-Peer Network. *IACR Cryptol. ePrint Arch.* 2018 (2018), 236. <http://eprint.iacr.org/2018/236>
 - [37] Yuval Marcus, Ethan Heilman, and S. Goldberg. 2018. Low-Resource Eclipse Attacks on Ethereum’s Peer-to-Peer Network. *IACR Cryptol. ePrint Arch.* 2018 (2018), 236.
 - [38] Billy Markus and Jackson Palmer. 2013. Dogecoin.
 - [39] Petar Maymounkov and David Mazières. 2002. Kademlia: A Peer-to-Peer Information System Based on the XOR Metric. In *IPTPS (Lecture Notes in Computer Science, Vol. 2429)*. Springer, 53–65.
 - [40] Andrew Miller, James Litton, Andrew Pachulski, Neal Gupta, Dave Levin, Neil Spring, and Bobby Bhattacharjee. 2015. Discovering bitcoin’s network topology and influential nodes. *University of Maryland, Tech. Rep* (2015).
 - [41] Alan Mislove, Massimiliano Marcon, Krishna P. Gummadi, Peter Druschel, and Bobby Bhattacharjee. 2007. Measurement and Analysis of Online Social Networks. In *Proceedings of the 7th ACM SIGCOMM Conference on Internet Measurement* (San Diego, California, USA) (IMC '07). Association for Computing Machinery, New York, NY, USA, 29–42. <https://doi.org/10.1145/1298306.1298311>
 - [42] Satoshi Nakamoto. 2009. Bitcoin: A peer-to-peer electronic cash system,” <http://bitcoin.org/bitcoin.pdf>.
 - [43] Till Neudecker. 2019. *Characterization of the Bitcoin Peer-to-Peer Network (2015-2018)*. Technical Report 1. Karlsruher Institut für Technologie (KIT). <https://doi.org/10.5445/IR/1000091933>
 - [44] Till Neudecker, Philipp Andelfinger, and Hannes Hartenstein. 2015. A simulation model for analysis of attacks on the Bitcoin peer-to-peer network. In *IM*. IEEE, 1327–1332.

- [45] Till Neudecker, Philipp Andelfinger, and Hannes Hartenstein. 2016. Timing Analysis for Inferring the Topology of the Bitcoin Peer-to-Peer Network. In *UIC/ATC/ScalCom/CBDCoM/IoP/SmartWorld*. IEEE Computer Society, 358–367.
- [46] Till Neudecker and Hannes Hartenstein. 2019. Network Layer Aspects of Permissionless Blockchains. *IEEE Commun. Surv. Tutorials* 21, 1 (2019), 838–857. <https://doi.org/10.1109/COMST.2018.2852480>
- [47] Colin Percival and Simon Josefsson. 2016. The scrypt Password-Based Key Derivation Function. *RFC 7914* (2016), 1–16. <https://doi.org/10.17487/RFC7914>
- [48] Kevin Roose. 2017. Is There a Cryptocurrency Bubble? Just Ask Doge., <https://www.nytimes.com/2017/09/15/business/cryptocurrency-bubble-doge.html>.
- [49] M. Saad, V. Cook, L. Nguyen, M. T. Thai, and A. Mohaisen. 2019. Partitioning Attacks on Bitcoin: Colliding Space, Time, and Logic. In *2019 IEEE 39th International Conference on Distributed Computing Systems (ICDCS)*. 1175–1187. <https://doi.org/10.1109/ICDCS.2019.00119>
- [50] Muhammad Saad, Jeffrey Spaulding, Laurent Njilla, Charles A. Kamhoua, Sachin Shetty, DaeHun Nyang, and David A. Mohaisen. 2020. Exploring the Attack Surface of Blockchain: A Comprehensive Survey. *IEEE Commun. Surv. Tutorials* 22, 3 (2020), 1977–2008.
- [51] Jimmy Song. 2017. *Bitcoin Cash: What You Need to Know*. Retrieved 1 Feb 2021 from <https://jimmysong.medium.com/bitcoin-cash-what-you-need-to-know-c25df28995cf>
- [52] Daniel Stutzbach and Reza Rejaie. 2006. Understanding churn in peer-to-peer networks. In *Internet Measurement Conference*. ACM, 189–202.
- [53] Qawi K Telesford, Karen E Joyce, Satoru Hayasaka, Jonathan H Burdette, and Paul J Laurienti. 2011. The Ubiquity of Small-world Networks. *Brain Connectivity* 1, 5 (2011), 367–375.
- [54] M. Tran, I. Choi, G. J. Moon, A. V. Vu, and M. S. Kang. 2020. A Stealthier Partitioning Attack against Bitcoin Peer-to-Peer Network. In *2020 IEEE Symposium on Security and Privacy (SP)*. 894–909. <https://doi.org/10.1109/SP40000.2020.00027>
- [55] trinity.ethereum.org. 2021. *The Trinity Ethereum Client*. Retrieved 2 Feb 2021 from <https://trinity.ethereum.org>
- [56] Pauli Virtanen, Ralf Gommers, Travis E. Oliphant, Matt Haberland, Tyler Reddy, David Cournapeau, Evgeni Burovski, Pearu Peterson, Warren Weckesser, Jonathan Bright, Stéfan J. van der Walt, Matthew Brett, Joshua Wilson, K. Jarrod Millman, Nikolay Mayorov, Andrew R. J. Nelson, Eric Jones, Robert Kern, Eric Larson, C J Carey, İlhan Polat, Yu Feng, Eric W. Moore, Jake VanderPlas, Denis Laxalde, Josef Perktold, Robert Cimrman, Ian Henriksen, E. A. Quintero, Charles R. Harris, Anne M. Archibald, Antônio H. Ribeiro, Fabian Pedregosa, Paul van Mulbregt, and SciPy 1.0 Contributors. 2020. SciPy 1.0: Fundamental Algorithms for Scientific Computing in Python. *Nature Methods* 17 (2020), 261–272.
- [57] Liang Wang and Ivan Pustogarov. 2017. Towards Better Understanding of Bitcoin Unreachable Peers. *CoRR* abs/1709.06837 (2017). arXiv:1709.06837 <http://arxiv.org/abs/1709.06837>
- [58] Addy Yeow. [n.d.]. Bitnodes Network Crawler, <https://github.com/ayeowch/bitnodes>.
- [59] Ian Young. 2018. Dogecoin: A Brief Overview & Survey. *Available at SSRN 3306060* (2018).